1   **Allometric scaling impacts plasticity in biomass allocation, morphology and**

2   **anatomical traits due to above and belowground resource limitation in cultivated**

3   **sunflower (*Helianthus annuus* L.)**

4

5   Yan Wang[1,2], Lisa A. Donovan[1], Andries A. Temme[1*]

6   1. Department of Plant Biology, Franklin College of Arts and Sciences, The University of Georgia,

7   Athens, GA, USA

8   2. Department of Silviculture, School of Forestry, Northeast Forestry University, Harbin, Heilongjiang,

9   150040, China

10   *Corresponding author: atemme@uga.edu (+1 706 207 4020)

Abstract

- Under benign conditions, as plants grow, size dependent (allometric) scaling changes mass allocation between organs. In the face of resource stress plants grow less but also show plasticity in multiple trait categories, including biomass allocation, morphology and anatomy. The extent to which size dependent (allometric) vs active (beyond allometric) responses to resource limitations are consistent with expectations for increasing resource acquisition potential is poorly understood. Here we assess the impact of allometric scaling on the direction, magnitude and coordination of trait plasticity in response to light and/or nutrient limitations in cultivated sunflower (*Helianthus annuus*).

- We grew seedings of ten sunflower genotypes for three weeks in a factorial of light (50% shade) and nutrient (10% supply) limitation in the greenhouse and measured a suite of allocational, morphological and anatomical traits for leaves, stems, fine roots, and tap roots.

- Under resource limitation, more biomass was allocated to the organ capturing the most limiting resource, as expected. Allometric scaling accounted for a substantial portion of many trait responses, especially for anatomical traits. Allometric and active responses were generally aligned in the same direction and for specific leaf area and specific root length under light and nutrient limitation, respectively, this alignment contributed to more acquisitive trait values. However, traits not generally associated with resource limitation showed the greatest active adjustment, e.g. tap root and stem theoretical hydraulic conductance. Although light limitation triggered a more pronounced coordinated trait adjustment than nutrient limitation, factoring out allometric scaling clarified that active coordinated trait responses to both light and nutrient limitation were similar in scale but resource specific.

- The substantial contribution of allometric scaling to trait responses that are consistent with a functional increase in the uptake capacity of the most limiting resource suggests that both allometric and active trait adjustments need be considered as potentially adaptive.

- **Keywords:** allocation, morphology, anatomy, allometry, phenotypic plasticity, K_s, SLA, SRL

Introduction

42
43 The extent of plant trait adjustment in response to a changed environment is generally considered
44 as the plant's phenotypic plasticity (Nicotra *et al*., 2010; Valladares *et al*., 2007). According to theory
45 (Gedroc *et al*., 1996; Shippley & Mezianne 2002; Poorter *et al*., 2012; Robinson *et al*., 2010), this
46 plasticity serves to optimize/maximize the uptake of the most limiting resource (Bloom *et al*.,
47 1985;Chapin, 1991). For example, increased mass allocation to leaves under shade, or to roots under
48 nutrient limitation alleviates some of the stress caused by resource limitation (Shipley & Maziane,
49 2002; Sugiura & Tateno, 2011). However, since plants are inevitably smaller under resource stress, a
50 factor to consider in understanding these traits shifts under resource limitation is how allometric
51 scaling affects traits (McConnaughay & Coleman 1999; Onsas *et al*., 2013; Poorter et al. 2015; Reich
52 2002, 2018; Shipley & Meziane, 2002; Weiner 2004;).

53 Allometric scaling, as narrowly defined, governs the relationship between mass allocation at
54 differing plant parts (Weiner 2004). Across and within species this scaling relationship is such that
55 smaller plants allocate proportionally more mass to leaves than to roots (Poorter *et al*., 2015). Thus,
56 in shade, allometric scaling associated with a smaller plant under limiting resources could be seen as
57 a strategy to acquire the most limiting resource at a given plant size (Coleman *et al*., 1994; Müller *et
58 al*., 2000; Reich, 2002). This "passive" (Nicotra *et* al., 2010) or "apparent" (McConnaughay and
59 Coleman 1999) plasticity predisposes the plant to attune its traits with the available resources and
60 resource demand. However, there is evidence for active adjustments (adjustments beyond those
61 accounted for by allometry) that can affect resource uptake. For example, greater plant height for a
62 given mass under low light condition aids in light uptake (Rice & Bazzaz, 1989). The extent to which
63 plasticity in a broader range of trait responses (beyond just mass allocation) during resource
64 limitation is active vs an effect of size dependent (allometric) scaling is poorly understood.

65 Most research to date governing allometric scaling has focused on broad intraspecific comparisons
66 of species (Poorter *et al*. 2015). However, at the intraspecific level there could be population or
67 genotypic level differences in these scaling relationships. If responses due to allometric scaling and
68 active adjustments vary in the degree to which they align, and if this variation has a genetic
69 component, then within species and populations there could be variation in tolerating stress at
70 different points in the growth cycle. Moreover, "passive" adjustments in traits associated with size
71 cannot be a priori regarded as or ruled out as adaptive (cf Nicotra et al. 2010, Poorter et al. 2019). If
72 traits responses that are consistent with greater ability to take up the most limiting resource have
73 both allometric and active components, this suggests that the magnitude and alignment of both
74 components need to be considered when evaluating evidence for functional and putatively adaptive
75 responses.

76 Among plant traits, anatomical traits are often overlooked due to time and budget constraints.
77 However, variation in anatomical traits underlies or contributes to variation in morphological and
78 physiological traits that have received much attention (John *et al*., 2017; Kong *et al*., 2014; Scoffoni
79 *et al*., 2015). For example, palisade parenchyma thickness is positively correlated to leaf thickness
80 (Catoni *et al*., 2015) and photosynthetic rate (Chatelet *et al*., 2013). A thicker cortex could provide a
81 relative larger site for mycorrhizal infection and higher resource uptake in thicker roots, especially
82 for the arbuscular mycorrhiza (Kong *et al*., 2014). Root cortex thickness, due to the size of cortical
83 cells (Eissenstat & Achor, 1999) strongly affects fine root diameter (Gu *et al*., 2014; Guo *et al*., 2008).
84 Exploring how responses in anatomical traits align with those of other traits will enhance our
85 understanding of how plants adjust to changing environmental conditions from tissue, to organ, to
86 architecture.

87 Across species or populations within a species, plant functional traits are generally expected to
88 exhibit a coordinated shift due to resource limitation in their typical habitats, i.e., the leaf, stem, root
89 and whole-plant economics spectrum with acquisitive traits at high resource conditions (Díaz *et al.*,
90 2016; Fortunel *et al.*, 2012; Reich, 2014; Wright *et al.*, 2004;). Moreover, trait values are thought to
91 show a coordinated response across all organs, supporting the idea of a whole-plant-based strategy
92 (Reich, 2014). However, within species, much remains unclear about how the expectation of
93 integrated trait responses at the 'whole plant economic spectrum' (Reich, 2014) level plays out at
94 the level of environmentally induced plasticity. Especially in terms of coordination among a broad
95 set of traits and plant organs and how size induced, allometric, plasticity affects this.

96 To add to our understanding of plant response to resource limitation, here we examined trait
97 responses to light and nutrient limitation of traits across different trait categories (biomass
98 allocation, morphology and anatomy) and organs (leaf, stem and root) in cultivated sunflower. Prior
99 research has shown strong plastic responses to resource limitation and other environmental factors
100 in *Helianthus* (Bowsher *et al.*, 2017; Donovan *et al.*, 2014; Masalia *et al.* 2018; Temme *et al.*, 2019).
101 Specifically, we sought to answer the following questions:

> 1) How do mass allocation, organ morphology, and anatomy change with above and below
>   ground resource limitation, and what role does size scaling of traits play in this?
> 2) How do traits compare for magnitude of plasticity and what role does size scaling of traits
>   play in this?
> 3) Do traits show a coordinated shift due to resource limitation across all organs and what role
>   does size scaling of traits play in this?

Material and Methods

Experimental design

110 To address these questions we selected a set of 10 cultivated sunflower genotypes, varying broadly
111 in biomass based on prior work (**Table S1**) from a larger diversity panel used for genomic dissection
112 of traits (Mandel *et al.*, 2011; Masalia *et al.*, 2018; Nambeesan *et al.*, 2015). We conducted a
113 factorial design of two nutrient treatments (rich and poor) and two light treatments (sun and shade)
114 at the Botany greenhouses of The University of Georgia USA in March 2018. Achenes were sown in
115 seedling trays and allowed to grow for seven days, after which each seedling was transplanted to 5
116 liter (1.3 gallon) pot filled with a 3:1 sand:calcinated clay mixture (Turface MVP, Turface Athletics,
117 Buffalo Grove, IL). Pots were arranged in a split plot design of 6 replicate blocks or whole-plot. The
118 light treatment was applied as the whole-plot factor, with 2 sub-plots in each plot randomly assigned
119 to unshaded or 50% shade generated with high density woven polyethylene cloth (Fig. S1). Within
120 each subplot, two pots of each genotype were randomly distributed and supplied with either 40g or
121 4g fertilizer (Osmocote Plus 15-9-12 with micronutrients, Scotts, Marysville, OH, USA), totaling 240
122 pots (plants). Greenhouse temperature controls were set to maintain 18–24 °C, and supplemental
123 lighting was provided to maintain a 15/9-h photoperiod.

Plant harvest and trait measurements

125 Plants were harvested 3 weeks after transplanting (4 weeks after germination). At harvest, plant
126 height (from soil surface to top of apical meristem) and stem diameter (midway between cotyledons
127 and first leaf pair) were measured. Plants were separated into root, leaf (including cotyledons), and
128 stem (including bud if present—rarely) for organ anatomy, morphology and allocation
129 measurements. In order to determine the relative magnitude of adjustments to anatomy,
130 morphology and allocation traits we assigned all measured traits to one of these three categories.
131 While we believe our assignment of traits to categories is defensible, we acknowledge that this is

132   somewhat arbitrary and that different groupings could influence results associated with
133   comparisons among categories.

134   For plant anatomical traits, from each replicate plant, one recently matured fully expanded leaf was
135   sampled, cutting a 1×0.5 cm rectangle out of the leaf center, a 5 mm length stem segment (centered
136   between the cotyledon and the first leaf pair) was cut, a 1 cm tap root segment was cut 4 cm below
137   the root/stem junction, and from a single lateral root attached to the tap root near to the root/stem
138   junction with an intact root tip, a 1 cm fine root segment was cut 2 cm from the apex of the root. All
139   tissue subsamples were fixed in formalin–acetic acid-alcohol solution, FAA, (50% ethanol (95%), 5%
140   glacial acetic acid, 10% formaldehyde (37%) and 35% distilled water).

141   Fixed subsamples were processed for anatomy at the University of Georgia Veterinary Histology
142   Laboratory. Each sample was embedded and gradually infiltrated with paraffin, sliced with a sledge
143   microtome, mounted to a slide, and stained with safranin and fast green dye. Slides were imaged
144   with a camera mounted Zeiss light microscope using ZEN software (Carl Zeiss Microscopy,
145   Oberkochen, Germany). Cell (i.e., conduit) and tissue (i.e., palisade and spongy, cortex and vascular
146   or stele) dimensions of leaf, stem, fine and tap roots were traced using Motic Images Advanced 3.2
147   software (Motic Corporation, Xiamen, China). Theoretical hydraulic conductivity (Ks, $kg·s^{-1}·m^{-1}·MPa^{-1}$)
148   for each sample was calculated, based on the Hagen-Poiseuille equation (Tyree & Ewers, 1991): $ks =$
149    $(\pi\rho/128\eta Aw) \sum_{i=1}^{n} d_i^4$. where ρ is the density of water (988.3 $kg·m^{-3}$ at 20 °C); η is the viscosity of
150   water (1.002×10^{-9} MPa·s at 20 °C); Aw is the stele (vascular) cross-section area, d is the diameter of
151   the ith vessel and n is the number of conduits in the xylem.

152   For plant morphological traits, after anatomical trait samples were collected, the rest of the leaf,
153   stem, and fine/tap root of each plant were scanned (Espon, Expression1680, Japan). Total root
154   length and volume of fine root, tap root and stem, as well as leaf area were measured using
155   WinRhizo (v. 2002c, Regent Instruments, Quebec, Canada), respectively. Then, the subsamples were
156   dried at 60°C for 48 h and weighed. Specific leaf area (SLA, $cm^2·g^{-1}$) and specific root length (SRL, $m·g^{-1}$)
157   ^{1}) were calculated as the ratios of leaf area to leaf dry mass, and root length to root dry mass,
158   respectively. Tissue density ($g·cm^{-3}$) was calculated as the ratio of dry mass to volume for stem, tap
159   and fine root, respectively. Leaf dry matter content (LDMC, $mg·g^{-1}$), used as a proxy for leaf tissue
160   density, was measured as leaf dry mass divided by leaf fresh mass (Kramer-Walter *et al*., 2016;
161   Wilson *et al*., 1999).

162   For allocational traits, total plant dry mass was calculated as the sum of all plant parts, including the
163   subsamples for anatomical and morphological traits. Once anatomy and morphology subsamples
164   were collected, the remaining tissue organs were dried at 60°C for 48 h and weighed. Prior to fixed
165   in FAA, the fresh biomass of subsamples for anatomical analysis was measured and converted to dry
166   biomass based on the ratio of fresh/dry biomass of remaining tissue organs. Finally, the mass
167   fractions for each tissue were calculated as proportions of total plant dry mass ($g·g^{-1}$).

168   *Data analysis*
169   The statistical analysis for the phenotypic data was performed using R v3.5.1 (R Core Team). To
170   obtain genotype means from our split plot design, a mixed effects model was fitted using the
171   package *lme4* (Bates *et al*., 2018) with genotype, light and nutrient level and all their interactions as
172   fixed effects and light treatment within block as random factor. Least-square (LS) means of all trait
173   values without random factor were estimated from this model using the R package *emmeans* (Lenth
174   *et al*., 2018). To test the effect of genotype and treatment on measured traits we fitted a less
175   expansive mixed effects model with genotype, light and nutrient level as well as the interaction
176   between light and nutrient level as fixed effects (following Freschet *et al*., 2018) and light treatment

177 within block as random factor. From this model, fixed effects were then tested using a Walds Chi-
178 square test in a type III Anova using the package *car* (Fox *et al*., 2018). Differences between
179 treatments were tested using a Tukey test corrected for multiple comparisons. We then estimated
180 the influence of plant allometry on the significance of nutrient and light limitation effects on traits by
181 adding (log-transformed) plant biomass as a fixed factor to both models and recalculating means
182 and significance (Ryser & Eek, 2000; Wahl *et al*., 2001). The relative shift in trait value per genotype
183 was calculated as the value in control (high nutrient & unshaded conditions) minus that in each
184 treatment, and divided by the value at control.

185 To quantify the plastic response of each trait to each resource limitation treatment, we calculated
186 the relative distance plasticity index (RDPI, Valladares *et al*., 2006, Scoffoni *et al*., 2015) as
187 $(x_i' - x_i / x_i' + x_i)$, where x_i and x_i' are the mean trait values of genotypes grown under control
188 (high-light and high-nutrient) and resource limited condition. In addition, the RDPI for each traits and
189 resource limitation treatment was recalculated after correcting for plant size (total biomass).
190 Significant values of RDPI (difference from zero, no plasticity) were determined using T-test on
191 genotype averages.

192 A principal component analysis (PCA) was applied to the trait data before and after correcting for
193 size, to determine major sources of variation across multiple traits and identify whether there were
194 concerted trait adjustments to limitation in above or belowground resources. Differences between
195 treatments were tested using, Bonferroni corrected, Hotellings-t test on the first two principal
196 components. Data visualizations were made using *ggplot2* (Wickham *et al*., 2018).

Results

198 Across all genotypes, plant biomass decreased by 21.4%, 53.3%, and 65.8% under light, nutrient, and
199 combined limitation, respectively, with additive effects of both stresses on whole plant biomass (**Fig.**
200 **1a, Table 1**). Moreover, traits frequently scaled with biomass and genotypes differed in the effect of
201 biomass on trait value (**Table 1).**

202 *Allometric and active responses to resource limitation*
203 Allocational traits were affected in contrasting ways by above and belowground resource limitation.
204 The ratio of leaf mass to fine root mass (LFRratio) increased under light limitation (+82.6%) due to
205 both increased mass allocation to leaf mass (LMF, +3.7%) and decreased allocation to fine roots
206 mass (FineRMF, -41.4%). In contrast, LFRratio decreased under nutrient limitation (-45.7%) due to
207 decreased LMF (-12.1%) and an increased FineRMF (+71.4%). A significant interaction of light and
208 nutrient limitation was found on allocational traits, e.g., LMF, stem mass fraction (SMF) and FineRMF
209 (**Table 1**). After allometric scaling was taken into account by statistically correcting for the effect of
210 total plant dry mass on trait values, the effect of light limitation on leaf mass fraction disappeared,
211 indicating that the increased LMF response was largely driven by the reduction in plant size and not
212 an active adjustment to resource limitation (**Table 1**).

213 Light limitation affected all morphological traits except for fine root diameter (FRD) (**Table 1**). The
214 responses led to strong increases in acquisitive values for resource acquiring traits such as SLA
215 (+40.5%, **Fig. 2a**), SRL (fine root, +31.8%, **Fig. 2b**; tap root +86.9%), and a moderate increase in plant
216 height (Height, +15.0%) (**Table 2**). This was accompanied by strong decreases in organ dimensions,
217 e.g., leaf thickness (LT, -10.8%), stem diameter (SD, -18.02%), tap root diameter (TRD, -28.84%), as
218 well as tissue density assessed as leaf dry matter content (LDMC, -20.57%); stem tissue density (STD,
219 -22.89%), fine root tissue density (FineRTD, -18.76%). After allometric scaling was factored out, the
220 effect of light limitation on largely disappeared, indicating that the root trait adjustments were

221   mainly driven by allometric scaling (**Table 2**).

222   In contrast to the effect of light limitation, nutrient limitation affected only 4 out of 12
223   morphological traits (**Table 1**). Nutrient limitation decreased SD (-15.6%) and FRD (-7.3%), and
224   increased the fine root specific root length (FineSRL, +19.8%) (**Fig. 2b**, **Table 2**) and TapRTD (+16.6%,
225   **Table 2**). After allometric scaling was factored out, the effect of nutrient limitation on these traits
226   remained, indicating active adjustments.

227   Similar to allocational and morphological traits, responses of anatomical traits to resource limitation
228   were also organ-specific. Light limitation affected leaf, stem, and tap root anatomical traits, while
229   nutrient limitation predominately affected fine root traits. More specifically for light limitation,
230   aboveground traits responded by decreasing leaf palisade parenchyma layer thickness (LPT, -12.1%,
231   **Fig. 3a**), stem cortex thickness (SCT, -11.6%), stem vascular bundle thickness (SVT, -26.2%, **Fig. 3b**)
232   and stem xylem thickness (SXT, -24.7%) (**Table 2**). Belowground traits responded by reducing tap
233   root cortex thickness (TRCT, -12.9%) and stele diameter (TRSD, -33.6%) (**Table 2**). Vascular tissue
234   adjustment to light limitation led to changes in theoretical hydraulic conductivity, with for decreased
235   leaf hydraulic conductivity (LKs, -19.0%) but increased stem hydraulic conductivity (SKs, +32.4%)
236   (**Table 2**). After allometric scaling was factored out, the effect of light limitation on SCT, SVT, TRCT
237   and TRSD was driven mainly by allometric scaling (**Table 2**), but there was active adjustment for
238   greater stem and tap root hydraulic conductivity (SKs, +95.9%; TRKs, +94.1%) (**Table 2**).

239   In contrast to light limitation, nutrient limitation predominately affected fine root anatomy. Nutrient
240   limitation decreased fine root cortex thickness (FRCT, -7.72%, **Fig. 3c**) and fine root stele diameter
241   (FRSD, -7.95%) (**Table 2**). After allometric scaling was factored out, the effects of nutrient limitation
242   on FRCT remained in both light conditions, however the effect of nutrient limitation on FRSD
243   disappeared under low light condition (**Table 2**).

244   *Allometric and active trait plasticity*
245   Trait categories differed in magnitude and direction of plasticity depending on resource limitation
246   (**Fig. 4**). Based on simple means per category in absolute relative distance plasticity index (RDPI),
247   biomass allocational traits showed relatively larger magnitude in plasticity, followed by morphology,
248   and last anatomy (**Fig. 4a**). On average, light limitation induced a higher RDPI values than nutrient
249   limitation (**Fig. 4**). When allometric scaling is factored out, the average magnitude of RDPI values
250   decreased for most traits (**Fig. S2**). Notable exceptions were, plant height, SKs and TRKs, for which
251   RDPI increased after taking plant biomass into account indicating active and passive responses to be
252   in opposite directions **(Fig. 4b, Fig. S2).**

253   *Coordinated trait adjustment to resource limitation*
254   When the genotypes means for traits in all three traits categories (allocation, morphology, and
255   anatomy) and all treatments were included in a principal component analysis, the first two axis
256   explained 34.4% and 13.4% of the variation **(Fig. 5a).** Light and nutrient limitations moved the key
257   set of traits to be more acquisitive along the first and second axis, respectively, e.g., higher SLA
258   under shade, higher FineSRL under nutrient limitation **(Fig. 5a).** Overall, light limitation triggered
259   more pronounced coordinated trait adjustment than nutrient limitation (**Fig. 5a**). However, after
260   allometric scaling was factored out, active coordinated trait responses to both light and nutrient
261   limitation were more similar in scale and resource specific.

262 Discussion

263   Here we assessed the impact of allometric scaling on the direction, magnitude, and coordination of
264   allocation, morphological and anatomical trait responses to light or/and nutrient limitation in

265   cultivated sunflower. We found more biomass was allocated to the organs acquiring the most
266   limiting resource (roots for nutrient stress and leaves for shade) and that morphological and
267   anatomical trait adjustments generally led to more acquisitive trait values (higher SLA in shade and
268   higher SRL in nutrient stress). Although portions of the plant trait responses were accounted for by
269   allometric scaling (i.e., trait changes due lower biomass of stressed plants), there was additional
270   active adjustments of key traits beyond allometric scaling. Interestingly, traits that showed the
271   greatest active adjustment were traits that are not often discussed in relation to light or light or
272   nutrient limitation, namely tap root and stem theoretical hydraulic conductance. We found evidence
273   for coordination of both allometric and active adjustments for many traits in response to resource
274   stress.

275   *Plasticity and allometry*
276   Our results demonstrated that plants increase biomass allocation to the plant part acquiring the
277   most limiting resource, both through allometric scaling and additional active responses (Bloom *et al*.,
278   1985; Poorter *et al*., 2012). Lower light availability resulted in increased relative investment in
279   aboveground plant organs (higher LMF and SMF) and lower nutrient availability resulted in increased
280   relative investment in belowground (FineRMF). This allocation pattern has been confirmed in other
281   growth forms (e.g., grasses, Siebenkäs *et al*., 2015; shrubs, Valladares *et al*., 2000; trees, Reich *et al*.,
282   1998, Kramer-Walter & Laughlin, 2017). Both morphology and anatomy adjustments resulted in a
283   higher specific area of light and nutrient capture per biomass invested under each stress
284   respectively. Additionally, anatomical adjustments in leaf and root, both decreased LPT and FRCT,
285   reduce tissue metabolic and maintenance costs (Guo *et al*., 2006, Galindo-Castañeda *et al*., 2018;
286   Jaramillo *et al.*, 2013). Thus, greater capacity for resource acquisition was coupled with reduced
287   costs.

288   The relatively high SKs and TRKs in shaded plants was associated with the functional hydraulic
289   continuum with taller plants. Both plant height and SLA of shaded plants were significantly greater
290   than the control (**Tables 1, 2**), resulting in an increase in axial transportation distance and total
291   transpiring surface. Theoretical hydraulic conductance, SKs and TRKs of shaded plant were increased
292   by 95.9% and 94.1% when taking biomass into account indicating active adjustments beyond
293   allometry (**Table 2**). This suggests that a coordinated increase in axial above- and below-ground
294   hydraulic conductance offsets the greater transportation resistance (Plavcová & Hacke, 2012),
295   ensuring efficient movement of carbon to roots and nutrients and water to leaves (Maurel *et al*.,
296   2010; Rodríguez-Gamir *et al*., 2016; Wahl *et al*., 2001).

297   Besides a response to resource limitation, many traits showed a strong correlation with plant biomass
298   indicating allometric scaling, with larger plants having a thicker leaf, stem and tap root (**Table 1**).
299   Consistent with Poorter et al. 2012, we found that light limitation effects were more accounted for by
300   allometry then nutrient limitation effects. However, even when accounting for plant biomass by using
301   total biomass as a covariate, treatment effects remained significant for major traits, such as SLA,
302   FineSRL, LPT and FRCT, indicating active adjustments as well. This demonstrates that light and nutrient
303   limitation had substantial active effect on plant adjustments to the major morphological and
304   anatomical traits influencing resource acquisition indicate allometry. Generally, allometric
305   adjustments went in a similar direction as the active adjustments (**Fig 3**). Thus, both allometric scaling
306   as well as active trait adjustments were consistent with trait adjustments that serve to ameliorate
307   some of the effects of resource limitation.

308   *Magnitude of trait adjustments*
309   Consistent with other resource limitation studies, plasticity of mass allocational traits was largest,
310   followed by morphological traits (Kramer-Walter & Laughlin, 2017, Valladares *et al*., 2000), and

311   smallest in anatomical traits (Catoni *et al.*, 2015; Cai *et al.*, 2017; Xu *et al.*, 2015). It should be noted
312   that differences in the extent of plasticity for different categories of traits may be species specific or
313   based on the traits included. For example, oak (*Quercus robur)* seedlings were more plastic in
314   physiological traits under shade, yet beech (*Fagus sylvatica)* was more plastic in morphological traits
315   (Valladares *et al.*, 2002). Differences among trait categories for the magnitude of plasticity may
316   reflect an inherent hierarchy originating from the internal structural framework of any specific
317   organ. For example, leaf thickness is highly correlated with palisade parenchyma (Scoffoni *et al.,*
318   2015) and root diameter with cortex and/or stele thickness (Kong *et al.,* 2014). Thus, small shifts in
319   individual component anatomical traits could add up to larger shifts in morphological traits which in
320   turn affect allocational traits.

321   In general, pulling out allometric effects decreased the magnitude of morphological and anatomical
322   traits adjustment. Only the RDPIs of the plant height, SKs and TRKs increased especially under shade
323   when the allometry was accounted for (**Fig. 4, Fig. S2**). Given that height increased under shade, a
324   higher efficiency of stem and root transportation could offset greater resistance due to a longer
325   transportation distance (Plavcová & Hacke, 2012). It should be noted, however, that this increased
326   stem Ks may come at the cost of increased risk of xylem embolism in shaded plants (Tyree &
327   Zimmermann, 2002). However, the opposite response in leaf Ks provides a puzzling counterpoint
328   that would be worth assessing in more experiments. Additionally, the anatomical dataset collected
329   in this work provides an excellent resource for anatomical water flow models (Couvreur *et al.*, 2018)
330   to further shed light on the consequences of these anatomical trait adjustments for plant hydraulics.

331   *Trait coordination and resource strategy*
332   Contrary to the evolutionarily conservative strategy generally expected under low resource
333   conditions (Díaz *et al.,* 2016; Reich 2014), our results at the scale of environmentally induced
334   plasticity showed that traits shift towards values generally thought to be resource acquisitive under
335   stress (**Fig. 2-4; Table 1,2**), consistent with other resource manipulation studies for commonly
336   measured traits (Freschet et al. 2015). Our plants growing under lower resource conditions, with
337   lower biomass, had thinner leaves, stem, fine and tap roots, as well as narrower leaf palisade, stem
338   vascular tissue, fine root cortex and tap root stele, but higher SLA and SRL. These coordinated trait
339   shifts depended on the limiting resource or organ. For example, higher SLA and thinner LPT were
340   only significant under shade, while higher FineSRL and thinner FRCT and FRSD were only significant
341   under poor nutrient condition (**Table 2**). Thus, while there was some coordination, shifts were not
342   such that the resource use strategy at the whole-plant level shifted from conservative to acquisitive,
343   even though individual organs showed more acquisitive traits consistent with increased capture
344   ability for the limiting resource.

345   *Conclusion*
346   Few studies have assessed the phenotypic response of whole plants in terms of biomass allocation,
347   organ morphology and anatomy simultaneously, and even less under multiple resource limitation
348   (Givnish 1988; Pratt *et al.,* 2010). Here, our research demonstrates that major traits from all three
349   categories shift in response to resource limitation. The resource specific extent, direction, and
350   coordination of the responses is driven not only by changes in plant size (allometric scaling), but often
351   includes a variable amount of active adjustment that is sometimes, but not always, aligned in the same
352   direction as the allometric component. The substantial contribution of allometric scaling to trait
353   responses that are consistent with a functional increase in the uptake capacity of the most limiting
354   resource suggests that both allometric and active trait adjustments need be considered as potentially
355   adaptive.

356

Acknowledgements

Author contributions

YW, AT, and LD designed the experiment. YW carried out the experiment and took all measurements. YW and AT analyzed the results. YW wrote the initial manuscript draft with revisions by AT and LD. All authors contributed to manuscript revision, and read and approved the submitted version

Figure and table captions

Table 1 Allocational, morphological, and anatomical traits across a factorial of light and nutrient limitation. Light/Shade, direct sun vs 50% shade. Rich/poor, high nutrients vs 10% nutrient concentration. Means±SE of 10 genotypes estimated marginal mean (based on 5-6 replicates) from our split-plot design. Effects of genotype (G), light (L) and nutrient (N) stresses and their interactions (L×N) on plant traits data. With or without plant total biomass (Mass) as a covariate. ***:p<0.001, **:p<0.01, *:p<0.05, ns: not significant.

Table 2 Relative shift in allocational, morphological, and anatomical traits across a factorial of light and nutrient limitation. Light/Shade, direct sun vs 50% shade. Rich/poor, high nutrients vs 10% nutrient concentration. Means±SE of 10 genotypes relative shift in treat value as compared to Light-Rich treatment. Base values as measured and after correcting for the effect of biomass on trait value. Greyed out numbers are not significantly different from zero (T-test p>0.05).

Figure 1. Biomass and mass allocation of leaf, stem, tap root, and fine root tissue across a factorial of light and nutrient limitation. Light/Shade, direct sun vs 50% shade. Rich/poor, high nutrients vs 10% nutrient concentration. **(a)** Average whole plant biomass across genotypes (n=10), stacked by average tissue contribution. **(b)** Average mass allocation to tissue types per treatment. Error bars denote standard error across genotypes. Different letters represent significant (p<0.05) Tukey post hoc differences between treatments.

Figure 2. Leaf and fine root morphology across a factorial of light and nutrient limitation. Light/Shade, direct sun vs 50% shade. Rich/poor, high nutrients vs 10% nutrient concentration. **(a)** specific leaf area (SLA, $cm^2 g^{-1}$), **(b)** specific root length (SRL, $m g^{-1}$), **(c)** ratio of leaf area to root length (SLA/SRL, $cm^2 m^{-1}$). Points indicate genotype (n=10) mean (n=5-6) at a given treatment. Boxplots show distribution of values. Different letters represent significant (p<0.05) Tukey post hoc differences between treatments.

Figure 3. Leaf, stem, and fine root anatomy across a factorial of light and nutrient limitation. Light/Shade, direct sun vs 50% shade. Rich/poor, high nutrients vs 10% nutrient concentration. **(a)** leaf palisade parenchyma thickness (μm), **(b)** stem vascular bundle width (μm), **(c)** fine root cortex thickness (μm). Points indicate genotype (n=10) mean (n=5-6) at a given treatment. Boxplots show distribution of values. Different letters represent significant (p<0.05) Tukey post hoc differences between treatments

Figure 4. Trait plasticity in response to resource limitation. Points indicate the average (n=10) relative

399 distance plasticity index (RDPI) in response to light limitation (dark blue, Shade-Rich) or nutrient
400 limitation (light green, Light-Poor), or combined (light blue, Shade-Poor). Point size represents a T-test
401 significance (p<0.05) of RDPI being different from zero (large points) or not (small points). **(a)** RDPI
402 values taken from base measurements. **(b)** RDPI values when correcting trait values for biomass,
403 allometry. Trait abbreviations and units as in Table 1.

404 **Figure 5**. Principal component analysis (PCA) of leaf, stem and roots traits in response to resource
405 limation. Light/Shade, direct sun vs 50% shade. Rich/poor, high nutrients vs 10% nutrient
406 concentration. Panels represent **(a)** trait values as measured, **(b)** trait values after correcting for size
407 scaling (allometric effects). Different letters indicate significant Hotellings-T test, after Bonferroni
408 correction, between treatments on the first two principal components. Trait abbreviations and units
409 as in Table 1.

Supplementary materials

411 **Table S1.** List of genotypes used in this study, it's common name, the corresponding plant ID from the
412 USDA GRIN Database for each genotype, and the market type of each genotype.

413 **Fig S1**. Comparison of light levels between shaded and unshaded treatment. On average the low-light
414 treatment received 50% of the photon flux density of the high-light treatment. Light intensities in each
415 treatment were measured with a handheld light meter (LI-189; LI-COR, Lincoln, NE). Readings were
416 taken from 8:00 AM to 7:00 PM. The light sensor was held near the soil level in each plot. We
417 presented representative data from May 15th, a cloud-free day.

418 **Fig S2**. Effect of accounting for size scaling in traits when calculating relative distance plasticity index
419 (RDPI). RDPI changes are shown per treatment (Light/Shade, full sun/50% shade; Rich/Poor, full
420 nutrients/10% nutrients) and whether RDPI measures were positive or negative when initially
421 compared to control (Light-Rich). For positive RDPI values (traits that increase in trait value with stress)
422 a positive change when taking size scaling into account shows that size scaling decreased apparent (as
423 measured initially) plasticity (i.e taking size scaling into account shows increased plasticity). A negative
424 change on the other hand shows that the apparent plasticity was enhanced by size scaling (i.e taking
425 size scaling into account shows decreased plasticity. For negative RDPI values (traits that decrease in
426 trait value with stress) the effect of the sign of change is reversed. Symbols indicate whether RDPI
427 significance (different from zero) is gained (circles), lost (squares), or remains unchanged (triangles,
428 when taking biomass into account.

429 **Fig S3.** Scaling relationship between biomass and trait value among and between genotypes and
430 treatments. **(a)** Scaling relationships between individual plants per genotypes and treatment (dotted
431 lines) and **(b)** scaling relationships between genotypes per treatment.

References

Bates D, Maechler M, Bolker B, Christensen RHB, Singmann H, Dai B, Scheipl F, Grothendieck G, Green P. 2018. Package 'lme4'.

Bloom AJ, Chapin FS, Mooney HA. 1985. Resource limitation in plants - an economic analogy. *Annual Review of Ecology and Systematics* **16**: 363-392.

Bowsher AW, Shelby KC, Ahmed I, Krall E, Reagan DJ, Najdowski MN, Donovan LA. 2017. Genotype Rankings for Nutrient Stress Resistance are Unrelated to Stress Severity in Cultivated Sunflower (*Helianthus annuus* L.). *Journal of Agronomy and Crop Science* **203**(3): 241-253.

Cai Q, Ji C, Yan Z, Jiang X, Fang J. 2017. Anatomical responses of leaf and stem of *Arabidopsis thaliana* to nitrogen and phosphorus addition. *Journal of Plant Research* **130**(6): 1035-1045.

Catoni R, Gratani L, Sartori F, Varone L, Granata MU. 2015. Carbon gain optimization in five broadleaf deciduous trees in response to light variation within the crown: Correlations among morphological, anatomical and physiological leaf traits. *Acta Botanica Croatica* **74**(1): 71-94.

Chatelet DS, Clement WL, Sack L, Donoghue MJ, Edwards EJ. 2013. The evolution of photosynthetic anatomy in Viburnum (adoxaceae). *International Journal of Plant Sciences* **174**(9): 1277-1291.

Chapin FSI. 1991. Integrated responses of plants to stress a centralized system of physiological responses. *Bioscience* **41**(1): 29-36.

Coleman JS, McConnaughay KDM, Ackerly DD. 1994. Interpreting phenotypic variation in plants. *Trends in Ecology & Evolution* **9**(5): 187-191.

Coleman JS, McConnaughay KDM, Bazza KA. 1993. Elevated CO_2 and plant nitrogen-use: Is reduced tissue nitrogen concentration size- dependent. *Oecologia* **93**: 195-200.

Couvreur V, Faget M, Lobet G, Javaux M, Chaumont F, Draye X. 2018. Going with the flow: Multiscale insights into the composite nature of water transport in roots. *Plant Physiology* DOI:10.1104/pp.18.01006.

Díaz S, Kattge J, Cornelissen JHC, Wright IJ, Lavorel S, Dray S, Reu B, Kleyer M, Wirth C, Colin Prentice I, Garnier E, Bönisch G, Westoby M, Poorter H, Reich PB, Moles AT, Dickie J, Gillison AN, Zanne AE, Chave J, Joseph Wright S, Sheremet Ev SN, Jactel H, Baraloto C, Cerabolini B, Pierce S, Shipley B, Kirkup D, Casanoves F, Joswig JS, Günther A, Falczuk V, Rüger N, Mahecha MD, Gorné LD. 2016. The global spectrum of plant form and function. *Nature* **529**(7585): 167-171.

Donovan LA, Mason CM, Bowsher AW, Goolsby EW, Ishibashi CDA, Cornwell W. 2014. Ecological and evolutionary lability of plant traits affecting carbon and nutrient cycling. *Journal of Ecology* **102**(2): 302-314.

Eissenstat DM, Achor DS. 1999. Anatomical characteristics of roots of citrus rootstocks that vary in specific root length. *New Phytologist* **141**: 309-321.

Fort F, Cruz P, Lecloux E, Bittencourt De Oliveira L, Stroia C, Theau J, Jouany C. 2016. Grassland root functional parameters vary according to a community-level resource acquisition-conservation trade-off. *Journal of Vegetation Science* **27**: 749-758.

Fortunel C, Fine PVA, Baraloto C. 2012. Leaf, stem and root tissue strategies across 758 Neotropical tree species. *Functional Ecology* **26**: 1153-1161.

Fox J, Weisberg S, Price B, Adler D, Bates D, Baud-Bovy G, Bolker B, Ellison S, Firth D, Friendly M, Gorjanc G, Graves S, Heriberger R, Laboissiere R. 2018. Package 'car'.

Freschet GT, Swart EM, Cornelissen JHC. 2015. Integrated plant phenotypic responses to contrasting above- and below-ground resources: Key roles of specific leaf area and root mass fraction. *New Phytologist* **206**: 1247-1260.

Freschet GT, Violle C, Bourget MY, Scherer-Lorenzen M, Fort F. 2018. Allocation, morphology, physiology, architecture: The multiple facets of plant above- and below-ground responses to resource stress. *New Phytologist* **219**(4): 1338-1352.

Galindo-Castañeda T, Brown KM, Lynch JP. 2018. Reduced root cortical burden improves growth and grain yield under low phosphorus availability in maize. *Plant, Cell & Environment* **41**: 1579-1592.

Givnish TJ. 1988. Adaptation to sun and shade: A Whole-Plant perspective. *Australian Journal of Plant Physiology* **15**: 63-92.

483 **Gu J, Xu Y, Dong X, Wang H, Wang Z. 2014.** Root diameter variations explained by anatomy and
484   phylogeny of 50 tropical and temperate tree species. *Tree Physiology* **34**(4): 415-425.
485 **Guo D, Xia M, Wei X, Chang W, Liu Y, Wang Z. 2008.** Anatomical traits associated with absorption and
486   mycorrhizal colonization are linked to root branch order in twenty-three Chinese temperate tree
487   species. *New Phytologist* **180**(3): 673-683.
488 **Hill JO, Simpson RJ, Moore AD, Chapman DF. 2006.** Morphology and response of roots of pasture
489   species to phosphorus and nitrogen nutrition. *Plant and Soil* **286**(1-2): 7-19.
490 **Jaramillo RE, Nord EA, Chimungu JG, Brown KM, Lynch JP. 2013.** Root cortical burden influences
491   drought tolerance in maize. *Annals of Botany* **112**(2): 429-437.
492 **John GP, Scoffoni C, Buckley TN, Villar R, Poorter H, Sack L. 2017.** The anatomical and compositional
493   basis of leaf mass per area. *Ecology Letters* **20**(4): 412-425.
494 **Kong D, Ma C, Zhang Q, Li L, Chen X, Zeng H, Guo D. 2014.** Leading dimensions in absorptive root trait
495   variation across 96 subtropical forest species. *New Phytologist* **203**(3): 863-872.
496 **Kramer-Walter KR, Bellingham PJ, Millar TR, Smissen RD, Richardson SJ, Laughlin DC. 2016.** Root
497   traits are multidimensional: Specific root length is independent from root tissue density and the
498   plant economic spectrum. *Journal of Ecology* **104**(5): 1299-1310.
499 **Kramer-Walter KR, Laughlin DC. 2017.** Root nutrient concentration and biomass allocation are more
500   plastic than morphological traits in response to nutrient limitation. *Plant and Soil* **416**(1-2): 539-
501   550.
502 **Lenth R, Singmann H, Love J, Buerkner P, Herve M, Abd Allah EF. 2018.** Package 'emmeans'.
503 **Mandel JR, Dechaine JM, Marek LF, Burke JM. 2011.** Genetic diversity and population structure in
504   cultivated sunflower and a comparison to its wild progenitor, *Helianthus annuus* L. *Theoretical and
505   Applied Genetics* **123**(5): 693-704.
506 **Masalia RR, Temme AA, Torralba NDL, Burke JM. 2018.** Multiple genomic regions influence root
507   morphology and seedling growth in cultivated sunflower (*Helianthus annuus* L.) under well-
508   watered and water-limited conditions. *PLoS One* **13**(9): e204279.
509 **Maurel C, Simonneau T, Sutka M. 2010.** The significance of roots as hydraulic rheostats. *Journal of
510   Experimental Botany* **61**(12): 3191-3198.
511 **Müller I, Schmid B, Weiner J. 2000.** The effect of nutrient availability on biomass allocation patterns
512   in 27 species of herbaceous plants. *Perspectives in Plant Ecology, Evolution and Systematics* **3**(2):
513   115-127.
514 **Nambeesan SU, Mandel JR, Bowers JE, Marek LF, Ebert D, Corbi J, Rieseberg LH, Knapp SJ, Burke JM.
515   2015.** Association mapping in sunflower (*Helianthus annuus* L.) reveals independent control of
516   apical vs. Basal branching. *BMC Plant Biology* **15**(1):84.
517 **Nicotra AB, Atkin OK, Bonser SP, Davidson AM, Finnegan EJ, Mathesius U, Poot P, Purugganan MD,
518   Richards CL, Valladares F, van Kleunen M. 2010.** Plant phenotypic plasticity in a changing climate.
519   *Trends in Plant Science* **15**(12): 684-692.
520 **Niinemets Ü, Kahru A, Mander Ü, Nõges P, Nõges T, Tuvikene A, Vasemägi A. 2017.** Interacting
521   environmental and chemical stresses under global change in temperate aquatic ecosystems: Stress
522   responses, adaptation, and scaling. *Regional Environmental Change* **17**(7): 2061-2077.
523 **Pilote. 2017. Ecological and evolutionary patterns among stem and leaf functional traits in
524   *Helianthus*.** The University of Georgia.
525 **Plavcov L, Hacke UG. 2012.** Phenotypic and developmental plasticity of xylem in hybrid poplar saplings
526   subjected to experimental drought, nitrogen fertilization, and shading. *Journal of Experimental
527   Botany* **63**(18): 6481–6491.
528 **Poorter H, Niklas KJ, Reich PB, Oleksyn J, Poot P, Mommer L. 2012.** Biomass allocation to leaves,
529   stems and roots: Meta-analyses of interspecific variation and environmental control. *New
530   Phytologist* **193**(1): 30-50.
531 **Poorter H, Niinemets Ü, Ntagkas N, Siebenkäs A, Mäenpää M, Matsubara S, Pons TL. 2019.** A meta-
532   analysis of plant responses to light intensity for 70 traits ranging from molecules to whole plant
533   performance. New Phytologist 223: 1073– 1105.

534 **Pratt RB, North GB, Jacobsen AL, Ewers FW, Davis SD. 2010.** Xylem root and shoot hydraulics is linked
535   to life history type in chaparral seedlings. *Functional Ecology* **24**(1): 70-81.
536 **Reich PB. 2014.** The world-wide 'fast-slow' plant economics spectrum: A traits manifesto. *Journal of*
537   *Ecology* **102**(2): 275-301.
538 **Reich PB. 2018.** Do plants increase resource acquisition potential in the face of resource shortfalls,
539   and if so, how? *New Phytologist* **219**(4): 1142-1144.
540 **Reich PB, Tjoelker MG, Walters MB, Vanderklein DW, Bushena C. 1998.** Close association of RGR, leaf
541   and root morphology, seed mass and shade tolerance in seedlings of nine boreal tree species grown
542   in high and low light. *Functional Ecology* **12**(3): 327-338.
543 **Rice SA, Bazzaz FA. 1989.** Quantification of plasticity of plant traits in response to light-intensity -
544   comparing phenotypes at a common weight. *Oecologia* **78**(4): 502-507.
545 **Rodríguez-Gamir J, Primo-Millo E, Forner-Giner MÁ. 2016.** An integrated view of Whole-Tree
546   hydraulic architecture. Does stomatal or hydraulic conductance determine whole tree
547   transpiration? *PLoS One* **11**(5): e155246.
548 **Robinson D, Davidson H, Trinder C, Brooker R. 2010.** Root–shoot growth responses during
549   interspecific competition quantified using allometric modelling. *Annals of Botany* **106**(6): 921-926.
550 **Ryser P, Eek L. 2000.** Consequences of phenotypic plasticity vs. Interspecific differences in leaf and
551   root traits for acquisition of aboveground and belowground resources1. *American Journal of*
552   *Botany* **3**(87): 402-411.
553 **Scoffoni C, Kunkle J, Pasquet-Kok J, Vuong C, Patel AJ, Montgomery RA, Givnish TJ, Sack L. 2015.**
554   Light-induced plasticity in leaf hydraulics, venation, anatomy, and gas exchange in ecologically
555   diverse Hawaiian lobeliads. *New Phytologist* **207**(1): 43-58.
556 **Shipley B, Meziane D. 2002.** The balanced-growth hypothesis and the allometry of leaf and root
557   biomass allocation. *Functional Ecology* **16**(3): 326-331.
558 **Siebenkaes A, Schumacher J, Roscher C. 2015.** Phenotypic plasticity to light and nutrient availability
559   alters functional trait ranking across eight perennial grassland species. *AoB Plants* **7**(plv029).
560 **Sugiura D, Tateno M. 2011.** Optimal Leaf-to-Root ratio and leaf nitrogen content determined by light
561   and nitrogen availabilities. *PLoS One* **6**(e222367).
562 **Sun Q, Yoda K, Suzuki S. 2005.** Internal axial light conduction in the stems and roots of herbaceous
563   plants. *Journal of Experimental Botany* **409**(56): 191-203.
564 **Temme AA, Liu JC, van Hal J, Cornwell WK, Cornelissena JHHC, Aerts R. 2017.** Increases in CO_2 from
565   past low to future high levels result in "slower" strategies on the leaf economic spectrum.
566   *Perspectives in Plant Ecology Evolution and Systematics* **29**: 41-50.
567 **Tyree MT, Ewers FW. 1991.** The hydraulic architecture of trees and other woody-plants. *New*
568   *Phytologist* **119**(3): 345-360.
569 **Tyree MT, Zimmermann MH** 2002**.** Xylem structure and the ascent of sap. *Springer Series in Wood*
570   *Science*: Springer, pp:229-235.
571 **Valladares F, Chico JM, Aranda I, Balaguer L, Dizengremel P, Manrique E, Dreyer E. 2002.** The greater
572   seedling high-light tolerance of *Quercus robur* over *Fagus sylvatica* is linked to a greater
573   physiological plasticity. *Trees-Structure and Function* **16**(6): 395-403.
574 **Valladares F, Gianoli E, Gómez JM. 2007.** Ecological limits to plant phenotypic plasticity. *New*
575   *Phytologist* **176**(4): 749-763.
576 **Valladares F, Sanchez-Gomez D, Zavala MA. 2006.** Quantitative estimation of phenotypic plasticity:
577   Bridging the gap between the evolutionary concept and its ecological applications. *Journal of*
578   *Ecology* **94**(6): 1103-1116.
579 **Valladares F, Wright SJ, Lasso E, Kitajima K, Pearcy RW. 2000.** Plastic phenotypic response to light of
580   16 congeneric shrubs from a Panamanian rainforest. *Ecology* **81**(7): 1925-1936.
581 **Violle C, Navas M, Vile D, Kazakou E, Fortunel C, Hummel I, Garnier E. 2007.** Let the concept of trait
582   be functional! *Oikos* **116**(5): 882-892.
583 **Wickham H, Chang W, Henry L, Pederson TL, Takahashi K, Wikle C, Woo K. 2018.** Package 'ggplot2'.

584   **Wilson PJ, Thompson K, Hodgson JG. 1999.** Specific leaf area and leaf dry matter content as
585   alternative predictors of plant strategies. *New Phytologist* **143**(1): 155-162.
586   **Wright IJ, Reich PB, Westoby M, Ackerly DD, Baruch Z, Bongers F, Cavender-Bares J, Chapin T,**
587   **Cornelissen JH, Diemer M, Flexas J, Garnier E, Groom PK, Gulias J, Hikosaka K, Lamont BB, Lee T,**
588   **Lee W, Lusk C, Midgley JJ, Navas ML, Niinemets U, Oleksyn J, Osada N, Poorter H, Poot P, Prior L,**
589   **Pyankov VI, Roumet C, Thomas SC, Tjoelker MG, Veneklaas EJ, Villar R. 2004.** The worldwide leaf
590   economics spectrum. *Nature* **428**(6985): 821-827.
591   **Xu N, Wang R, Liu J, Lu P, Guo W. 2015.** Hierarchy of plasticity traits in responses of *Quercus aliena* to
592   light conditions and water availability. *Dendrobiology* **74**: 169-180.
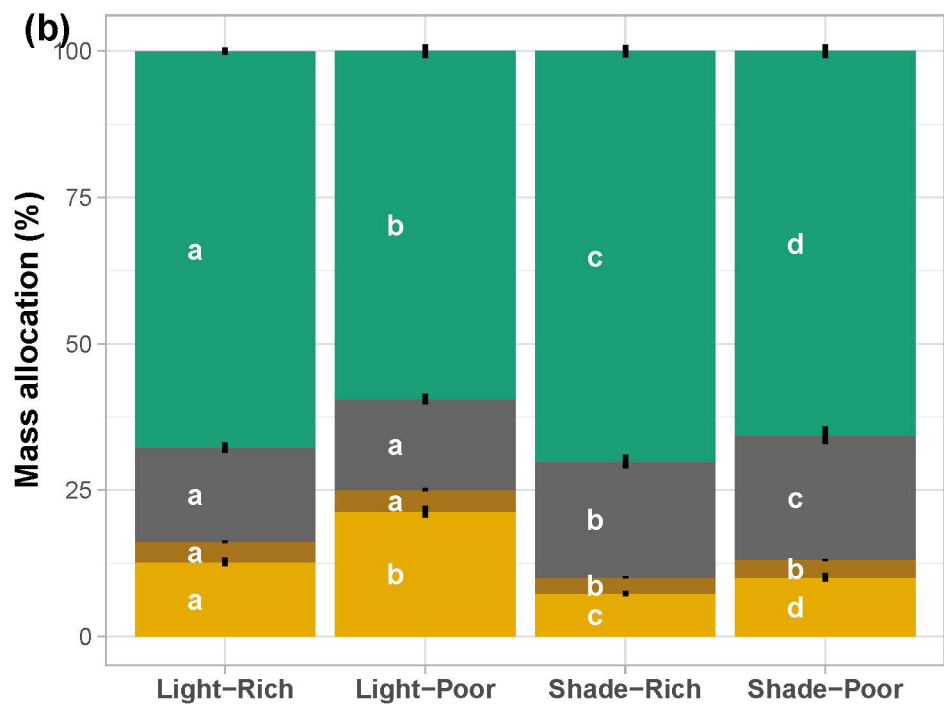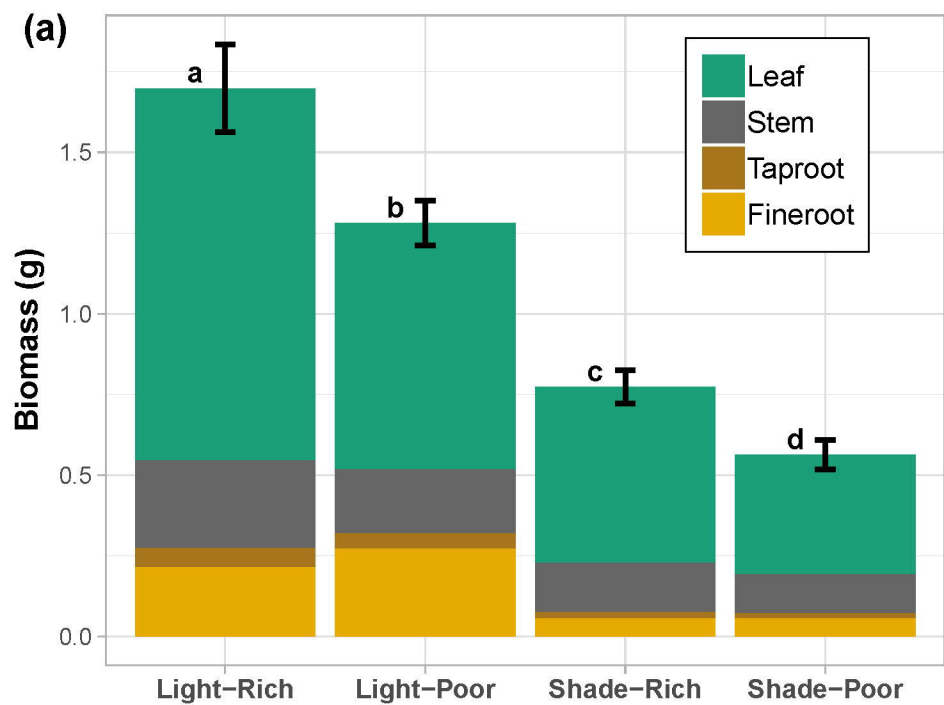593

594 **Table 1** Allocational, morphological, and anatomical traits across a factorial of light and nutrient limitation. Light/Shade, direct sun vs 50% shade. Rich/poor,
595 high nutrients vs 10% nutrient concentration. Means±SE of 10 genotypes estimated marginal mean (based on 5-6 replicates) from our split-plot design. Effects
596 of genotype (G), light (L) and nutrient (N) stresses and their interactions (L×N) on plant traits data. With or without plant total biomass (Mass) as a covariate.
597 ***:p<0.001, **:p<0.01, *:p<0.05, ns: not significant. Letters denote Tukey test post-hoc differences between treatments.
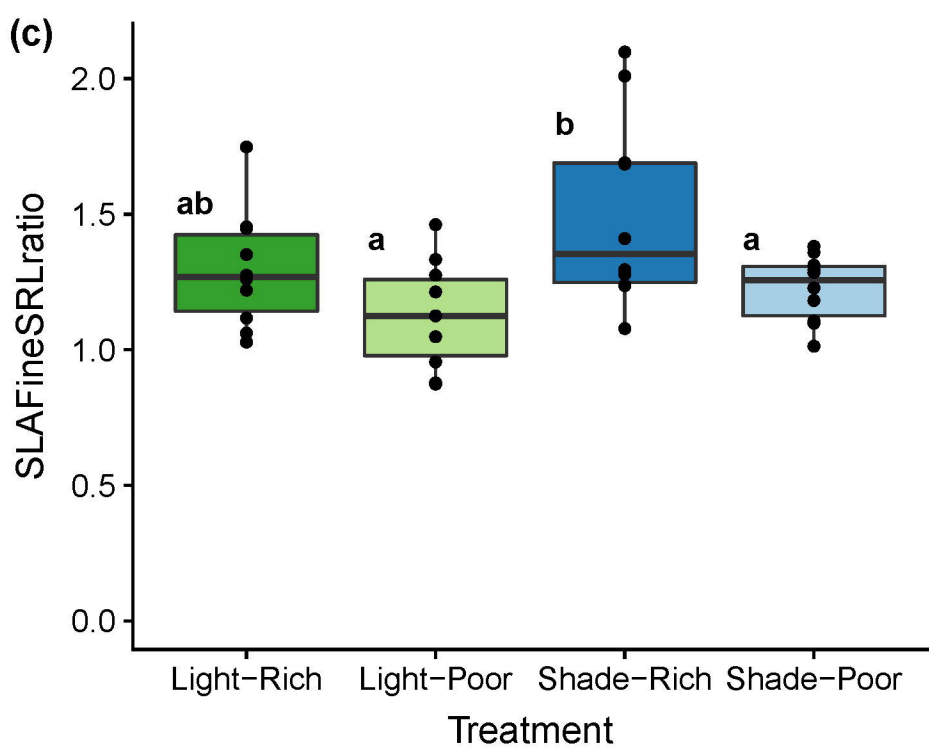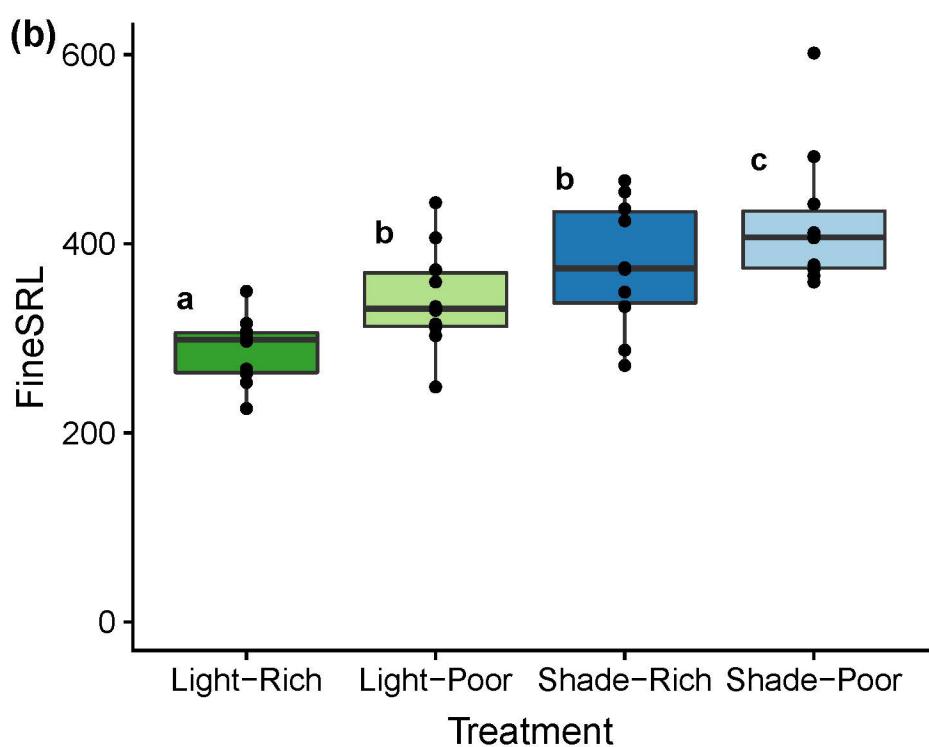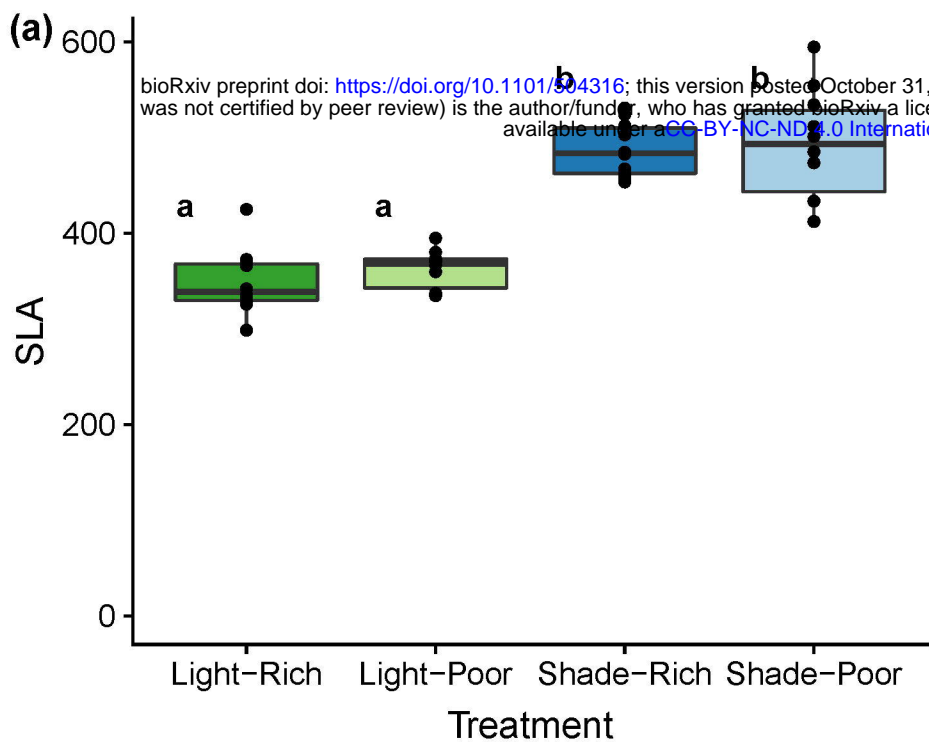
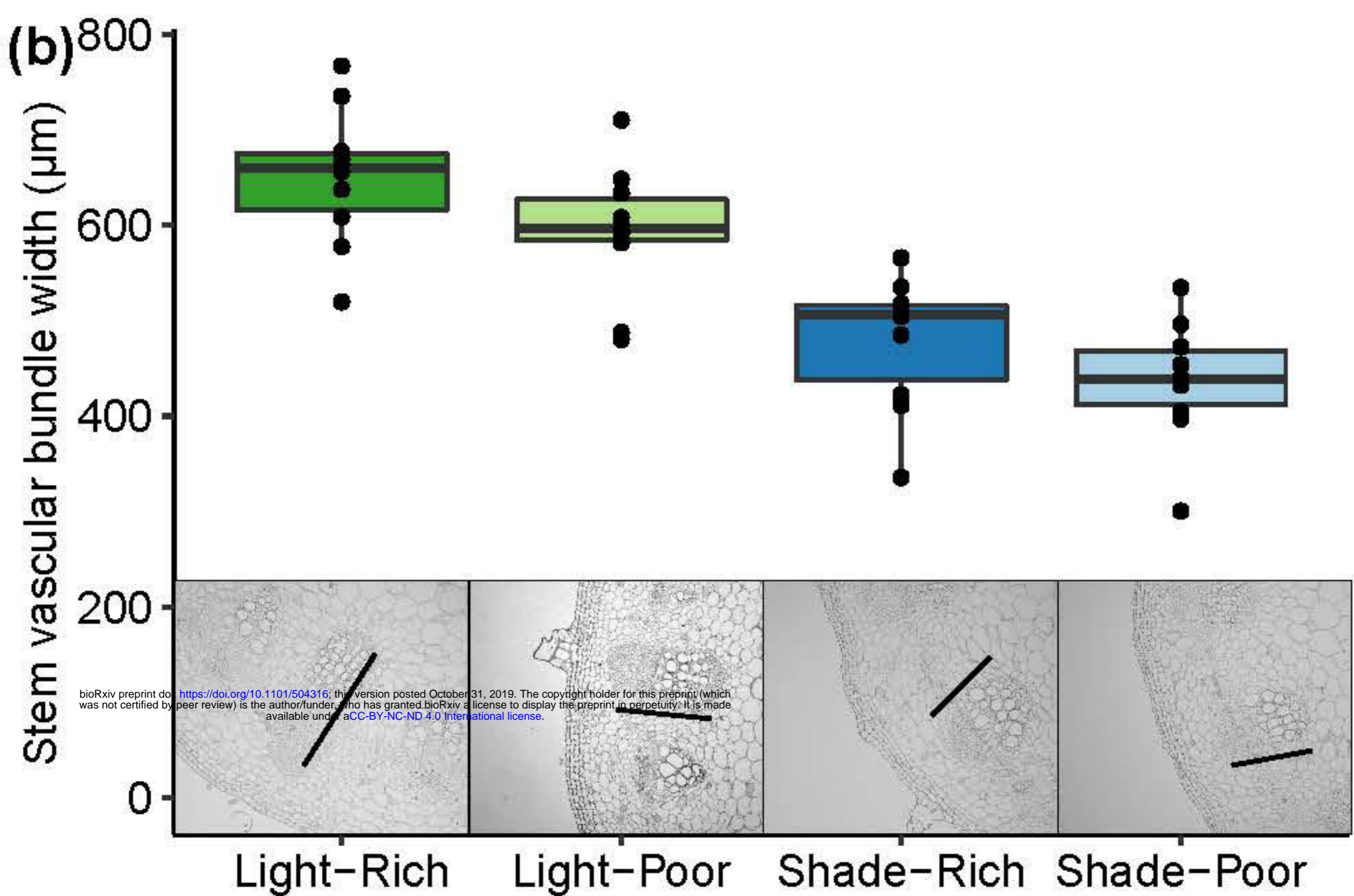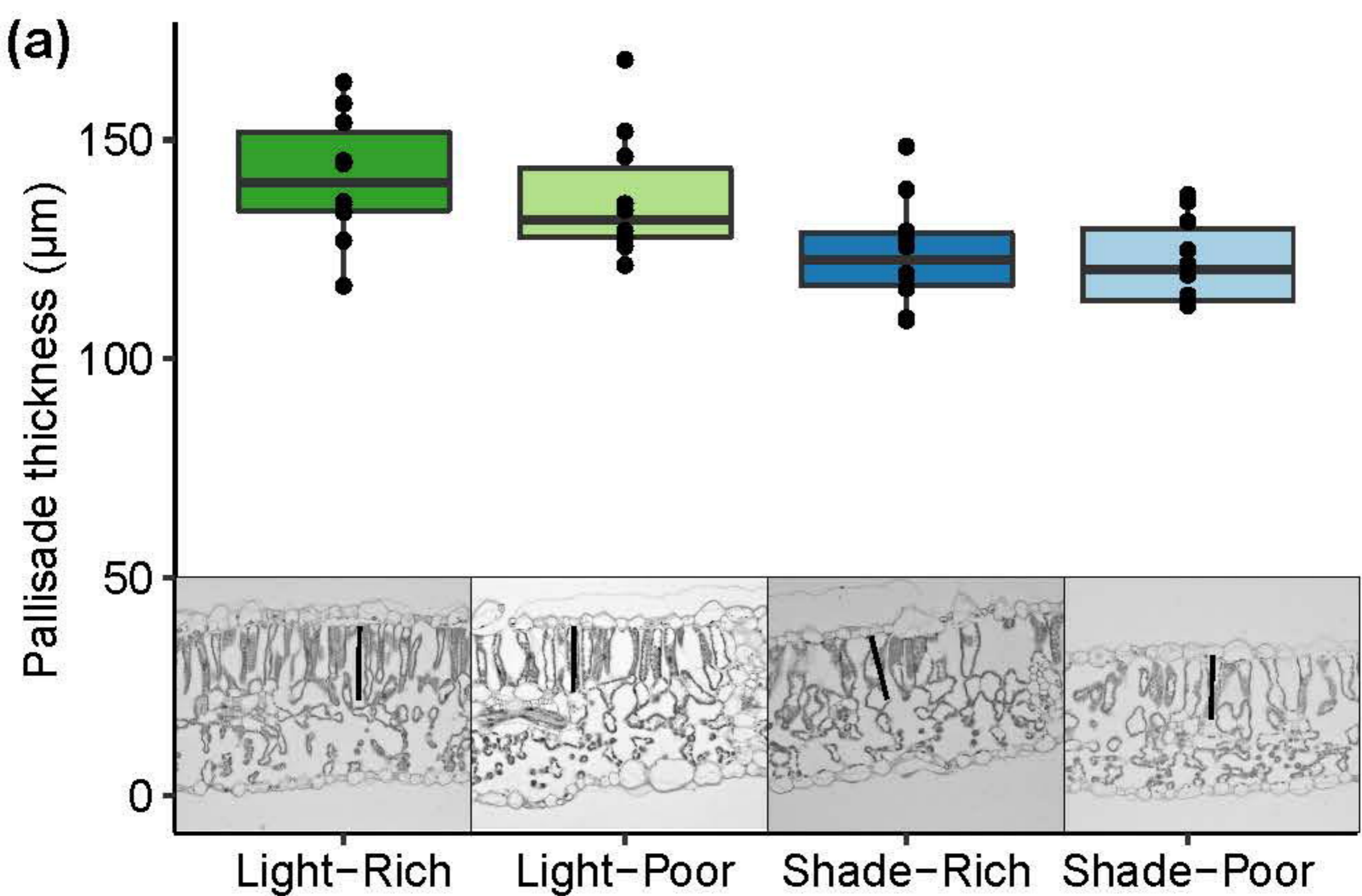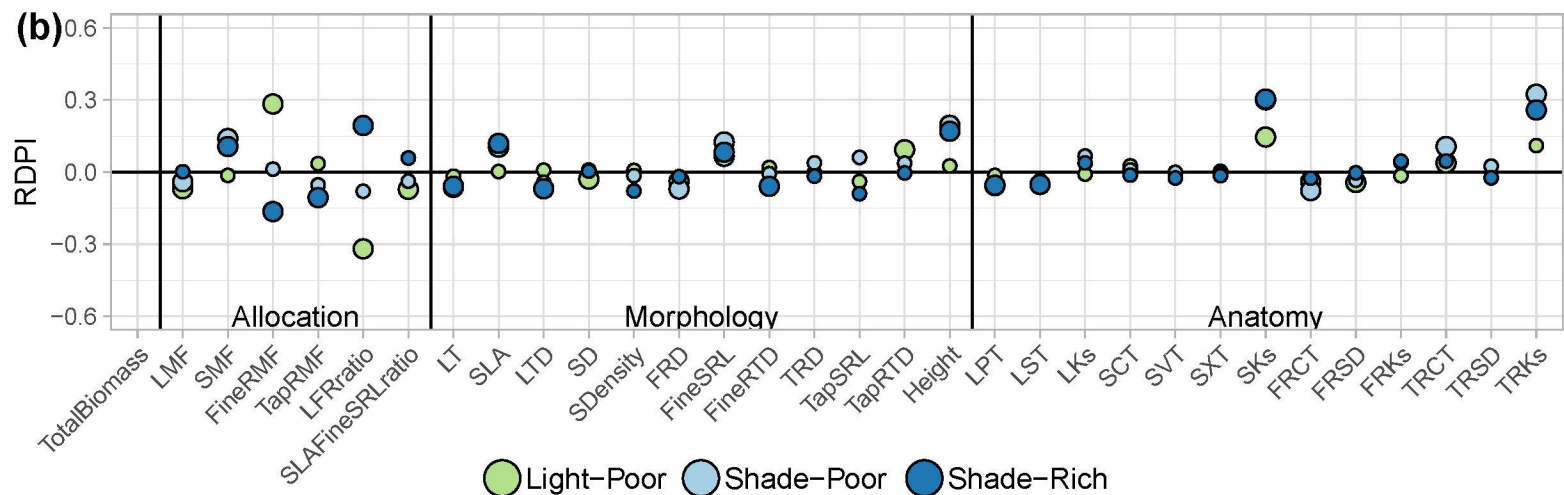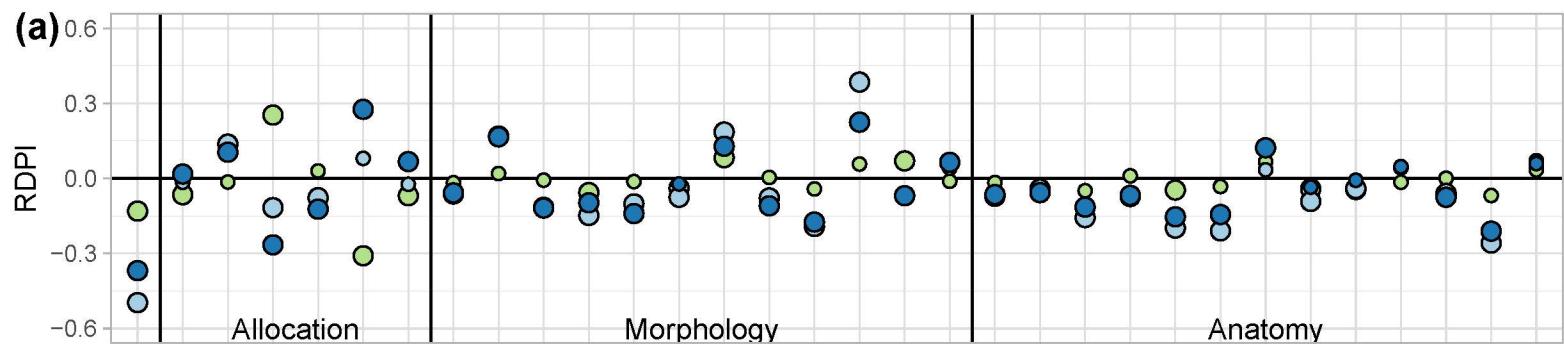| Category	Trait	Unit	Light-Rich	Light-Poor	Shade-Rich	Shade-Poor	Statistics G	L	N	L×N	-including biomass Mass	G	MxG	L	N	L×N
Allocation	Total Biomass	g	1.70±0.14[a]	1.28±0.07[b]	0.77±0.05[c]	0.56±0.05[d]	**	**	**	ns	n/a	n/a	n/a	n/a	n/a	n/a
	Leaf mass fraction	$g·g^{-1}$	0.68±0.006[a]	0.59±0.001[b]	0.70±0.01[c]	0.66±0.01[d]	**	**	**	**	ns	***	***	ns	***	***
	Stem mass fraction	$g·g^{-1}$	0.16±0.009[a]	0.16±0.009[b]	0.20±0.001[c]	0.21±0.02[b]	**	**	ns	*	ns	***	**	***	ns	**
	Fine root mass fraction	$g·g^{-1}$	0.13±0.007[a]	0.21±0.001[b]	0.074±0.004c	0.10±0.007[d]	**	**	**	**	ns	***	***	***	***	***
	Tap root mass fraction	$g·g^{-1}$	0.04±0.002[a]	0.04±0.003[b]	0.027±0.002[a]	0.03±0.002[b]	**	**	ns	ns	ns	***	ns	***	ns	ns
	Ratio of leaf and fine root		5.58±0.33[a]	2.93±0.22[b]	9.96±0.65[c]	6.58±0.40[a]	**	**	**	**	ns	***	ns	***	***	ns
	Ratio of SLA and FineSRL		1.30±0.07[ab]	1.13±0.06[b]	1.50±0.11[a]	1.23±0.04[b]	**	*	*	ns	ns	***	ns	*	ns	ns
Morphology	Leaf thickness	µm	257.71±8.38[a]	248.87±7.23[a]	228.86±4.75[a]	227.24±6.37[b]	**	**	ns	ns	*	***	ns	***	ns	ns
	Specific leaf area	$cm^2·g^{-1}$	349.53±11.04[a]	362.46±6.47[a]	487.72±8.96[b]	493.42±18.32[b]	**	**	ns	ns	**	***	ns	***	ns	ns
	Leaf dry mass content	$mg·g^{-1}$	102.95±2.66[a]	106.92±2.55[b]	87.33±2.78[a]	90.91±2.69[b]	ns	**	ns	ns	ns	***	ns	***	ns	ns
	Stem diameter	mm	5.23±0.18[a]	4.65±0.10[b]	4.30±0.13[c]	3.88±0.11[a]	**	**	**	ns	***	***	***	ns	***	***
	Stem tissue density	$g·cm^{-3}$	0.039±0.003a	0.037±0.002[b]	0.028±0.001[a]	0.031±0.002[ab]	*	**	ns	ns	ns	ns	ns	*	ns	ns
	Fine root diameter	µm	404.95±8.32[ac]	374.96±8.15[b]	388.27±1.95[c]	348.22±8.61[ab]	**	ns	**	ns	ns	***	ns	ns	**	ns
	Specific fine root length	$m·g^{-1}$	288.10±11.34[a]	342.28±17.57[b]	377.10±21.55[c]	423.75±23.45[a]	**	**	**	ns	ns	***	ns	*	*	ns
	Fine root tissue density	$g·cm^{-3}$	0.033±0.002[a]	0.033±0.001[b]	0.027±0.002[a]	0.028±0.001[ab]	**	**	ns	ns	ns	***	ns	ns	ns	ns
	Tap root diameter	µm	1337.49±62.57[a]	1228.76±59.19[b]	937.87±42.74[a]	900.58±36.41[b]	**	**	ns	ns	**	***	*	ns	ns	*
	Specific tap root length	$m·g^{-1}$	4.46±0.43[a]	5.04±0.56[b]	7.35±0.90[c]	10.51±2.06[ab]	**	**	ns	ns	*	*	ns	ns	ns	ns
	Tap root tissue density	$g·cm^{-3}$	0.037±0.002[a]	0.043±0.002[a]	0.033±0.002[b]	0.033±0.002[a]	**	**	**	*	ns	***	*	ns	***	*
	Height	cm	14.62±0.82[a]	14.33±0.93[b]	16.75±1.11[a]	16.43±1.64[b]	**	**	ns	ns	***	***	ns	***	*	ns
Anatomy	Leaf palisade thickness	µm	141.35±4.60[ac]	136.74±4.61[b]	124.16±3.96[c]	122.22±3.20[ab]	**	**	ns	ns	ns	***	ns	*	ns	ns
	Leaf spongy thickness	µm	79.96±4.93[ab]	74.11±4.63[b]	70.79±2.85[a]	73.60±4.85[ab]	**	**	*	*	*	***	*	**	*	*
	Leaf Ks	$kg·s^{-1}·m^{-1}·MPa^{-1}$	4.55±0.45[a]	4.27±0.53[b]	3.66±0.42[a]	3.34±0.33[ab]	**	**	ns	ns	ns	***	ns	ns	ns	ns
	Stem cortex thickness	µm	262.41±15.68[a]	266.45±12.93[b]	227.65±11.37[a]	225.16±10.32[b]	**	**	ns	ns	**	***	ns	ns	ns	ns
	Stem vascular thickness	µm	651.28±22.70[a]	593.58±21.77[b]	479.75±21.92[c]	436.78±19.99[d]	**	**	**	ns	***	***	*	**	ns	*
	Stem xylem thickness	µm	314.49±11.57[a]	293.74±7.17[a]	234.98±9.27[a]	205.33±8.60[c]	**	**	ns	*	***	***	ns	ns	ns	ns
	Stem Ks	$kg·s^{-1}·m^{-1}·MPa^{-1}$	8.62±0.77[ab]	9.86±0.89[a]	11.12±1.11[b]	9.56±1.09[ab]	**	**	ns	*	***	***	ns	***	**	ns
	Fine root cortex thickness	µm	136.38±2.99[a]	125.46±3.58[b]	127.44±4.13[a]	113.25±2.07[a]	*	ns	*	ns	ns	**	ns	ns	*	ns
	Fine stele diameter	µm	113.38±5.27[ab]	103.50±4.28[b]	111.68±5.01[a]	104.40±4.44[ab]	**	ns	**	ns	ns	***	ns	ns	*	ns
	Fine root Ks	$kg·s^{-1}·m^{-1}·MPa^{-1}$	0.54±0.07[a]	0.63±0.16[a]	0.66±0.15[a]	0.64±0.13[a]	**	ns	ns	ns	*	***	ns	ns	ns	ns
	Tap root cortex thickness	µm	209.14±8.67[a]	209.20±8.06[b]	182.66±13.98[a]	186.40±9.60[ab]	**	**	ns	ns	ns	***	ns	ns	ns	ns
	Tap root stele diameter	µm	888.75±60.60[a]	769.73±44.59[b]	569.64±22.97[c]	517.38±30.58[a]	**	**	**	ns	**	***	*	ns	ns	*
	Tap root Ks	$kg·s^{-1}·m^{-1}·MPa^{-1}$	27.16±4.14[a]	28.32±4.08[a]	29.43±3.84[a]	30.49±4.31[a]	**	ns	ns	ns	ns	***	ns	**	ns	ns

598

599 **Table 2** Relative shift in allocational, morphological, and anatomical traits across a factorial of light and nutrient limitation. Light/Shade, direct sun vs 50%
600 shade. Rich/poor, high nutrients vs 10% nutrient concentration. Means±SE of 10 genotypes relative shift in treat value as compared to Light-Rich treatment.
601 Base values as measured and after correcting for the effect of biomass on trait value. Greyed out numbers are not significantly different from zero (T-test
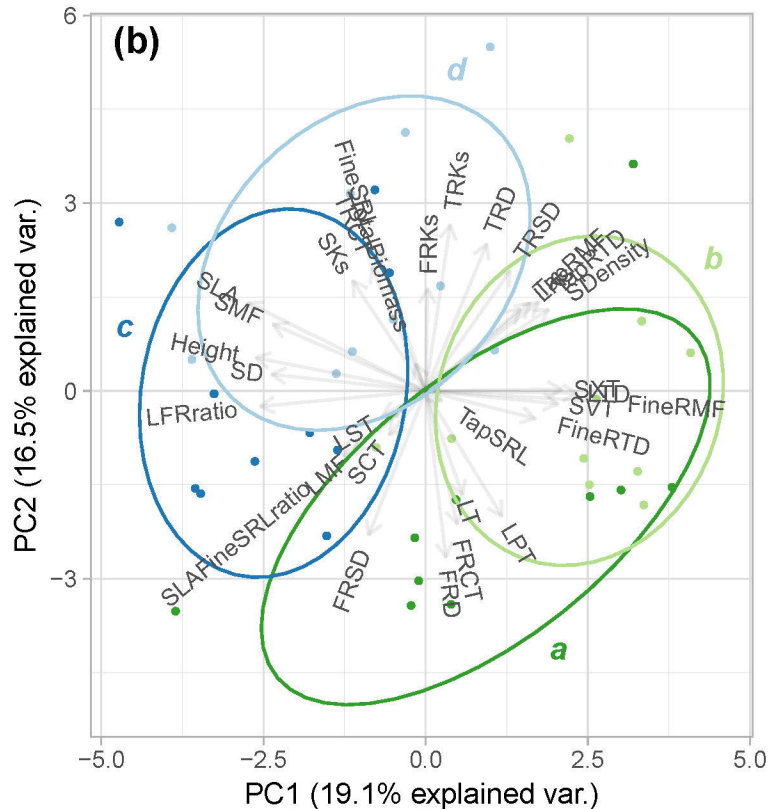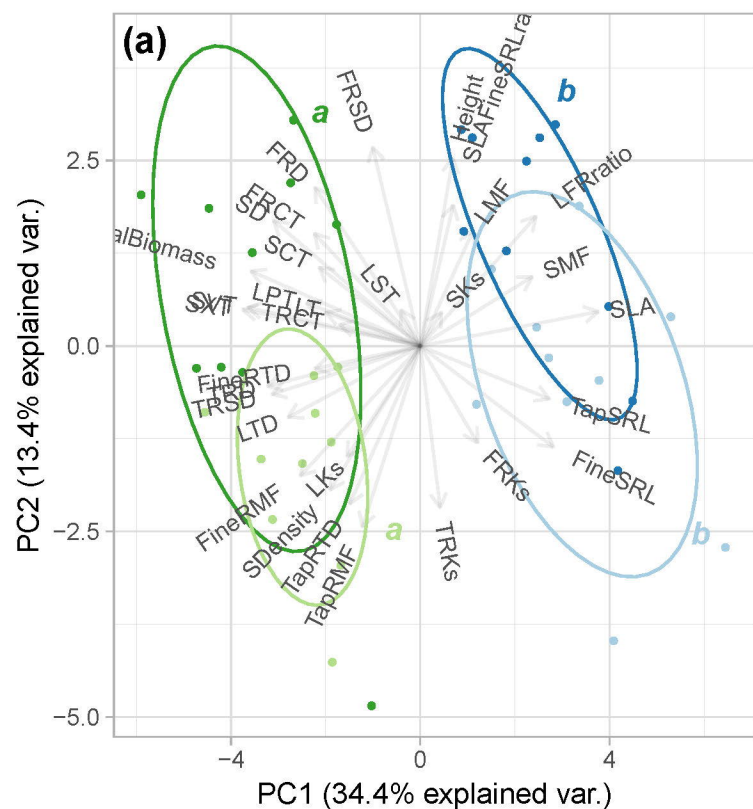602 p>0.05).

Category	Trait	Abreviation	Unit	Light-Poor		Shade-Rich		Shade-Poor	
				Base Δ%	Mass cor Δ%	Base Δ%	Mass cor Δ%	Base Δ%	Mass cor Δ%
Allocation	Total Biomass	TotalBiomass	g	-21.43±(5.94)		-53.25±(3.14)		-65.82±(2.81)	
	Leaf mass fraction	LMF	g·g^{-1}	-12.06±(1.97)	-12.85±(1.85)	3.67±(1.47)	0.37±(1.39)	-2.94±(1.88)	-7.62±(1.7)
	Stem mass fraction	SMF	g·g^{-1}	-2.07±(4.09)	-1.95±(4.08)	23.97±(3.81)	24.4±(3.8)	32.92±(5.55)	33.57±(5.53)
	Fine root mass fraction	FineRMF	g·g^{-1}	71.42±(10.45)	84.47±(12.91)	-41.36±(3.29)	-27.23±(4.67)	-19.59±(5.56)	4.82±(7.78)
	Tap root mass fraction	TapRMF	g·g^{-1}	6.81±(3.73)	7.92±(3.72)	-21.21±(3.7)	-18.49±(3.87)	-12.85±(5.86)	-8.57±(6.07)
	Ratio of leaf and fine root	LFRratio		-45.65±(5.3)	-47.15±(4.95)	82.61±(13.59)	53.12±(11.61)	20.81±(8.55)	-12.25±(7.04)
	Ratio of SLA and FineSRL	SLAFineSRLratio		-12.1±(4.1)	-12.59±(4.04)	16.35±(6.65)	14.37±(6.73)	-3.39±(4.77)	-6.12±(4.66)
Morphology	Leaf thickness	LT	mm	-3.11±(2.33)	-3.16±(2.33)	-10.8±(1.64)	-10.98±(1.63)	-11.47±(2.1)	-11.73±(2.1)
	Specific leaf area	SLA	cm^2·g^{-1}	4.25±(2.36)	0.85±(2.84)	40.53±(4.17)	27.59±(3.34)	42.24±(6.03)	24.2±(4.83)
	Leaf dry mass content	LTD	mg·g^{-1}	-0.69±(3.82)	2.47±(4.22)	-20.57±(3.42)	-12.26±(3.92)	-19.82±(4.36)	-7.12±(4.97)
	Stem diameter	SD	mm	-15.6±(3.82)	-11.26±(2.55)	-18.02±(3.42)	0.25±(2.77)	-27.56±(3.96)	-1.15±(2.57)
	Stem tissue density	SDensity	g·cm^{-3}	-0.21±(6.89)	3.96±(7.23)	-22.89±(5.73)	-12.55±(6.33)	-17.62±(4.13)	-1.74±(4.94)
	Fine root diameter	FRD	mm	-7.25±(1.85)	-7.1±(1.82)	-3.91±(3.02)	-3.32±(3.01)	-13.82±(2.15)	-12.96±(2.11)
	Specific fine root length	FineSRL	m·g^{-1}	19.82±(6.72)	15.72±(6.44)	31.81±(7.99)	19.58±(6.31)	50.35±(13.43)	32.56±(11.54)
	Fine root tissue density	FineRTD	g·cm^{-3}	2.22±(5.63)	5.59±(6.3)	-18.76±(4.39)	-10.31±(4.38)	-13.92±(3.33)	-0.44±(4.35)
	Tap root diameter	TRD	mm	-6.2±(6.59)	1.13±(6.2)	-28.84±(4.18)	-1.62±(6.83)	-31.25±(4.05)	9.52±(6.25)
	Specific tap root length	TapSRL	m·g^{-1}	16.66±(10.54)	-1.91±(11.5)	86.92±(35.39)	-7.72±(13.43)	163.95±(39.39)	25.7±(18.47)
	Tap root tissue density	TapRTD	g·cm^{-3}	16.56±(5.96)	22.11±(6.1)	-11.38±(6.17)	0.99±(6.59)	-9.65±(5.94)	9.51±(6.55)
	Height	Height	cm	-0.28±(6.84)	6.26±(4.95)	15.04±(5.91)	41.59±(4.38)	11.95±(9.83)	50.23±(7.5)
Anatomy	Leaf palisade thickness	LPT	mm	-2.95±(2.64)	-2.43±(2.63)	-12.05±(1.28)	-10.27±(1.3)	-13.1±(2.23)	-10.49±(2.18)
	Leaf spongy thickness	LST	mm	-7±(3.2)	-6.74±(3.24)	-10.34±(2.82)	-9.42±(2.85)	-7.61±(3.53)	-6.26±(3.56)
	Leaf Ks	LKs	kg·s^{-1}·m^{-1}·MPa^{-1}	-8.09±(4.91)	0.01±(6.03)	-19.02±(5.46)	9.59±(6.3)	-25.09±(6.07)	18.45±(9.99)
	Stem cortex thickness	SCT	mm	3.82±(6.52)	6.77±(6.05)	-11.57±(4.97)	-1.25±(5.33)	-12.06±(5.51)	3.39±(6.16)
	Stem vascular thickness	SVT	mm	-8.7±(2.17)	-1.97±(2.65)	-26.2±(2.78)	-4.41±(2.89)	-32.68±(2.93)	0.41±(3.59)
	Stem xylem thickness	SXT	mm	-5.83±(3)	0.83±(2.32)	-24.69±(3.24)	-2.39±(3.52)	-34.18±(2.98)	-1±(3.07)
	Stem Ks	SKs	kg·s^{-1}·m^{-1}·MPa^{-1}	17.4±(8.3)	39.01±(11.45)	32.36±(10.82)	95.94±(17.02)	19.83±(18.39)	107.23±(29.44)
	Fine root cortex thickness	FRCT	mm	-7.72±(2.86)	-7.26±(2.86)	-5.9±(4.28)	-4.18±(4.3)	-16.43±(2.97)	-13.93±(2.94)
	Fine stele diameter	FRSD	mm	-7.95±(3.29)	-7.75±(3.26)	-1.14±(2.58)	-0.35±(2.55)	-7.31±(3.07)	-6.14±(3.07)
	Fine root Ks	FRKs	kg·s^{-1}·m^{-1}·MPa^{-1}	14.42±(26.24)	14.31±(26.19)	30.55±(24.63)	30.06±(24.56)	17.28±(15.36)	16.67±(15.32)
	Tap root cortex thickness	TRCT	mm	0.77±(3.86)	8.32±(3.17)	-12.93±(5.06)	11.5±(7.25)	-10.59±(3.93)	24.66±(4.63)
	Tap root stele diameter	TRSD	mm	-10.47±(7.24)	-1.01±(9.76)	-33.64±(4.96)	-0.47±(11.43)	-39.98±(4.24)	9.48±(11.54)
	Tap root Ks	TRKs	kg·s^{-1}·m^{-1}·MPa^{-1}	9.34±(7.58)	34.04±(18.67)	18.56±(11.35)	94.08±(32.24)	21.85±(12.56)	128.2±(40.12)

603

(a)

Biomass (g)

Legend:
- Leaf
- Stem
- Taproot
- Fineroot

x-axis categories: Light–Rich, Light–Poor, Shade–Rich, Shade–Poor

Significance letters above bars: a, b, c, d

(b)

Mass allocation (%)

Significance letters within bars:
- Light–Rich: a (Leaf), a (Stem), a (Taproot), a (Fineroot)
- Light–Poor: b (Leaf), a (Stem), a (Taproot), b (Fineroot)
- Shade–Rich: c (Leaf), b (Stem), b (Taproot), c (Fineroot)
- Shade–Poor: d (Leaf), c (Stem), b (Taproot), d (Fineroot)

x-axis categories: Light–Rich, Light–Poor, Shade–Rich, Shade–Poor

(a)

(b)

(c)

Light-Rich ● Light-Poor ● Shade-Rich ● Shade-Poor